

Molecular Desorption of a NEG St 707 Irradiated at Room Temperature with Synchrotron Radiation of 194 eV Critical Photon Energy

F. Le Pimpec, O. Gröbner, J.M. Laurent
CERN, 1211 Geneva 23, Switzerland

11th March 2003

Abstract

Photon stimulated molecular desorption from a NEG St 707[®] (SAES GettersTM) surface after conditioning and after saturation with isotopic carbon monoxide¹, ¹³C¹⁸O, has been studied on a dedicated beam line at the EPA ring at CERN. The synchrotron radiation of 194 eV critical energy and with an average photon intensity of $\sim 1 \cdot 10^{17}$ photons.s⁻¹ was impinging on the sample at perpendicular incidence. It is found that the desorption yields η (molecules/photon) of the characteristic gases in an UHV system (hydrogen, methane, carbon monoxide and carbon dioxide) for a freshly activated NEG and for a NEG fully saturated with ¹³C¹⁸O are lower than that of 300 °C baked stainless steel.

1 Introduction

Non evaporable getters (NEG) have been used with great success for the vacuum system of the Large Electron Positron (LEP) collider at CERN during its operational period of over 10 years and have thus been instrumental in achieving and maintaining low pressures in a low conductance vacuum system typical for many high energy particle accelerators. In spite of the outstanding success of the continuous distributed NEG pumps in LEP, surprisingly little work has been done, at the start of this study [2], to understand photon or electron stimulated molecular desorption from such getter surfaces and their dependence on the surface saturation with adsorbed gas molecules [3] [4].

For the next generation accelerator at CERN, the Large Hadron Collider (LHC), it is also planned to make extensive use of getter pumping. Even though most of the LHC vacuum system (approx. 23 km) will be at cryogenic temperature and therefore will depend on cryo-pumping molecules at the wall of the cold beam pipe, the remaining 4 km at room temperature constitute a real challenge to the vacuum engineer. To obtain more complete data and a better understanding of the performance of a getter surface under realistic accelerator conditions, a test program has been started at CERN. This study was using an existing synchrotron radiation (SR) beam line for photon stimulated desorption (PSD) measurements and a laboratory system for electron stimulated desorption (ESD) [2] [5]. In this paper the work on PSD will be reported.

For practical reasons the commercially available and widely used NEG St 707[®] CTAM/30D (Zr 70%, V 24.6%, Fe 5.4%) [6] [7] ribbons from SAES GettersTM have been used. The SR spectrum of the photon beam line was characterized by a critical photon energy of 194 eV, hence slightly larger than the photon spectrum which will be emitted in the arcs of the LHC (44.3 eV). In order to be able to distinguish between the desorption process of molecules diffusing from the bulk and molecules pumped on the surface by a controlled saturation, isotopic carbon monoxide has been used. Indeed, saturating the surface with ¹³C¹⁸O instead of “conventional” carbon monoxide (CO or ¹²C¹⁶O), should allow a differentiation between the molecules deposited on the surface and pre-existing ¹²C¹⁶O coming from the bulk. Furthermore, the isotopic carbon monoxide could be used as a tool to find out whether carbon monoxide molecules dissociate [8] [9] on the surface and recombine with other atomic species present on the surface before being desorbed. Unfortunately the gas supply which was available for these measurements was of insufficient purity since it contained significant admixtures of “normal” C and O, cf §2.

¹cf nomenclature in [1]

2 Experimental Setup

The photodesorption yields (PSD yields) were measured using a multi purpose synchrotron radiation beam line at EPA (Electron Positron Accumulator) at CERN, as shown in Figure 1. The average photon flux impinging on the target was $\sim 1 \cdot 10^{17}$ photons. s^{-1} with a 194 eV critical energy. The insertion of a square collimator (12.3 x 12.3 mm) into the photon beam defines a divergence of 7.8 mrad and attenuates low energy photons (≤ 4 eV) in the vertical plane.

The gas flux desorbed during the irradiation is measured through an orifice with a conductance of 73.5 l/s for $^{12}C^{16}O$. This conductance divides the system into two parts. We will refer to these parts as : the target chamber, extending from the NEG chamber labelled St 707 in Figure 1 up to the conductance and secondly as the pumping chamber from the orifice up to the collimator.

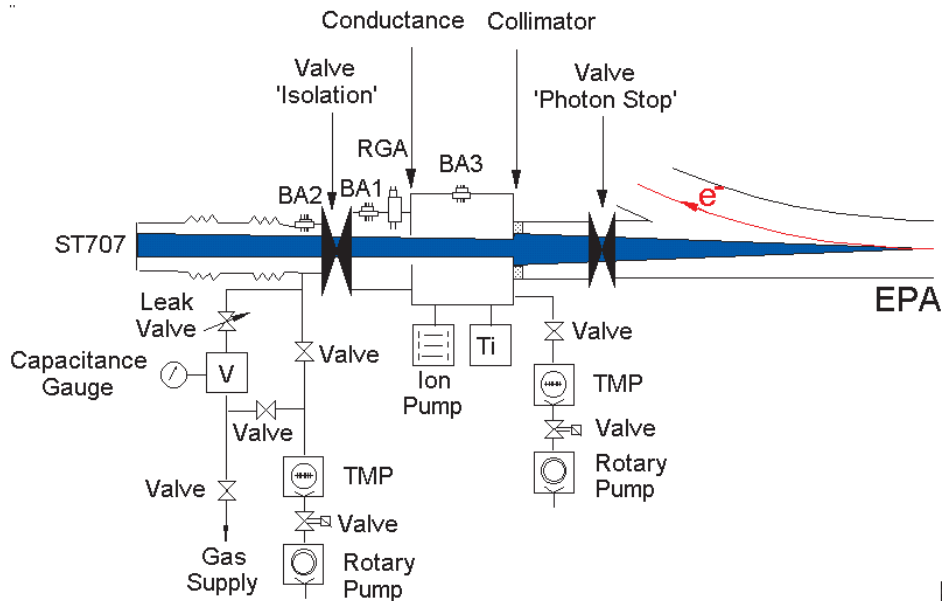


Figure 1: Experimental setup

The pressure is monitored by three calibrated Bayard Alpert gauges (type SVT 305), labeled BA1, BA2 and BA3 and a quadrupole mass analyser (RGA, Balzers QMG 112), Figure 1. The gas used for saturating the NEG or calibrating the RGA are injected through a baked gas injection line and tank. The purity of the gases contained in the bottles are of 99.997%. However, the isotopic carbon monoxide bottle contained a proportion of 94 atom % ^{13}C and 97 atom % ^{18}O . A more detailed description of the experimental setup can be found in [2].

Prior to their installation in the set-up, the elements supporting the NEG target, made of stainless steel (AISI 316 LN), were chemically cleaned according to a standardized procedure [10] and then vacuum fired at 950 °C for 2 hours. Subsequently the NEG strip was mounted onto the end flange of the stainless steel chamber which is 10 cm long and 6 cm in diameter, as shown in Figure 2.

In order to avoid irradiation of the stainless steel walls either by direct or by scattered radiation, additional NEG stripes were inserted on the wall of the cylindrical tube in front of the target, labelled Sleeve in Figure 2.

All irradiations were carried out at normal incidence, whereby about 23% (~ 6.5 cm 2) of the end face of the NEG chamber was directly irradiated. However, scattered light and photoelectrons may impinge on the 202 cm 2 exposed NEG surface. A small fraction of this scattered photon flux can also escape from the target and desorb gas from other parts of the beam line, thus perturbing the measurement. It could be shown, however, that this parasitic desorption is negligible for all targets except for the fully activated NEG [2]. In this latter case, the ratio between the hydrogen flux desorbed from the fully activated NEG target compared to the parasitic flux is approximately 2 [2].

The directly exposed area has been derived from the beam line parameters and was experimentally checked by observing the SR light falling on a screen placed on a view port mounted temporarily in place

of the CF 113.5 end flange, cf Figure 2. After this verification, the target was mounted at the position labeled St 707 in Figure 1. The estimation and the experimental check are in agreement to within 5%.

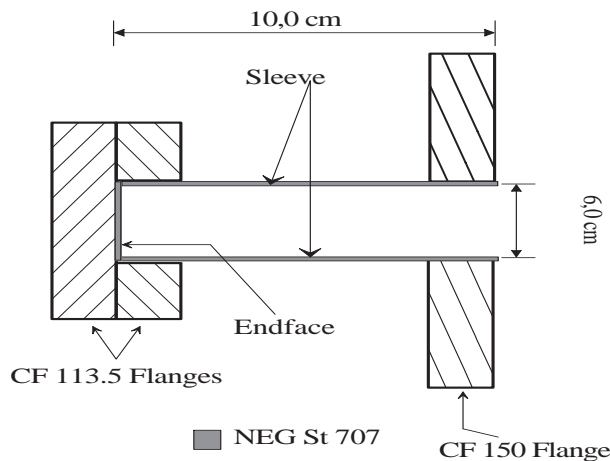


Figure 2: NEG target with an Endface and a Sleeve

3 Molecular Desorption

Prior to presenting the method used to measure the number of molecules desorbed, it might be of interest to the reader to have a very quick overview of DIET (Desorption Induced by Electronic Transition) which includes ESD [11] [12] and PSD processes [13] [14].

Both for ESD or PSD the direct momentum transfer between electrons or photons and molecules is a very inefficient process to induce molecular desorption and, if any, happen only in the first monolayer of the surface. Explanations for the desorption are attributed to the excitation of the adsorbed molecules via a mechanism involving an electron or hole of the substrate. From [15], it is also not excluded that subsurface layers contribute to the desorption signal. In this case, the question is whether or not this molecules or ions can travel through and escape the surface ?

The determination of the PSD yield η (molecules desorbed / incident photon) and the method used to calculate the integrated number of molecules desorbed during irradiation have been described in [2].

The expression of the PSD yield is given by equation(1). The flux of gas desorbed during irradiation is derived from the difference of the pressures on both sides of the known conductance, Figure 1. Using the definition of desorption coefficient η and by satisfying the condition that the pressure in the pumping chamber should always be much smaller than the pressure in the NEG chamber, one obtains the following equation :

$$\eta \approx G \frac{C \Delta P_{NEG}}{\dot{\Gamma}} \quad (1)$$

Where :

$\dot{\Gamma}$ is the flux of photons impinging on the target per second.

C is the conductance in l.s^{-1} for each gas species.

G is a constant, converting gas quantities (Torr.l) to number of molecules ($\sim 3.2 \cdot 10^{19}$ at 300K).

ΔP_{NEG} is the pressure increase in the NEG chamber measured during photon irradiation.

The total number of molecules desorbed during the entire irradiation period is obtained by integrating the partial pressures with respect to the time :

$$N_T = \int_0^{t_{off}} \eta \dot{\Gamma} dt = \int_0^{t_{off}} G C \Delta P_{NEG} dt \quad (2)$$

between the start and the end of the irradiation t_{off} .

In this experimental system the presence of hot filaments may induce thermal gas desorption from the surrounding surfaces. A measurement carried out at 300 K gives an outgassing flux of 10^{-9} Torr.l.s $^{-1}$

for hydrogen. This flux, if not corrected for, determines a lower measurement limit for η of $3.2 \cdot 10^{-7}$ hydrogen molecules / photon.

The provision of a large pumping speed (a Ti sublimator of 1000 l/s for H₂ and an ion pump of 200 l/s for N₂) and the use of a known conductance ensure the validity of equation (1). During exposure to the SR, the pressure BA3 in the pumping chamber was at least 3 times lower than the pressure measured by the reference gauge BA1.

The results, presented in §5, have been corrected for the background pressures which correspond to the partial pressures recorded by the RGA before the irradiations. The photon flux Γ was derived from the recorded machine parameters in EPA.

4 Experimental Programme

The experiments were carried out according to the following schedule :

1. Bakeout of the bare stainless steel chamber and of the whole setup, for 24 hours at 300 °C. The base pressure of the cool down beamline before irradiation were for BA1 $8 \cdot 10^{-11}$ Torr, and for BA3 $2 \cdot 10^{-11}$ Torr. The label of this irradiation is *Eta SS*.
2. Venting of the system up to the isolation valve. Installation of the NEG St 707 target. Pumping down and bakeout of the target chamber, except the NEG target, at 150 °C for 8 hours. During this period the NEG would reach a temperature of at most 30 °C. The NEG was irradiated “as received”. The base pressures before irradiation were for BA1 $3 \cdot 10^{-9}$ Torr, and for BA3 10^{-10} Torr. The label of this experiment is *NEG 0%*.
3. The NEG was then fully activated at 400 °C for ~45 min [6] [7] and was irradiated at room temperature. The base pressures were $8 \cdot 10^{-11}$ Torr for BA1 and $3 \cdot 10^{-11}$ Torr for BA3. The label of this experiment is *NEG 100%*.
4. Lastly the NEG was saturated with ¹³C¹⁸O by exposing it to a pressure of ~0.5 Torr for 8 hours. The base pressures after the pump down and before irradiation were $5 \cdot 10^{-10}$ Torr for BA1 and $3 \cdot 10^{-11}$ Torr for BA3. This experiment is called *NEG Sat (C13O18)*.

5 Results

Figures 3 to 7 represent the photodesorption coefficients of each gas species for the different experiments. Figure 8 displays the total number of carbon monoxide molecules, normal and isotopic, desorbed during the irradiation.

During all the irradiation the temperature, recorded on the outside of the target, on the sleeve and at the endface did not increase above 27°C and 28°C respectively.

The notation *C*O will refer to carbon monoxide molecules indistinctly of the combination of normal and isotopic C and O. We will use this notation when we will take into account all the species of carbon monoxide desorbed during irradiation.

In the legends of the plots, Figures 6 to 8, *CO* refers to ¹²C¹⁶O, *C13O* to ¹³C¹⁶O and *CO18* to ¹²C¹⁸O . *NEG Sat (C13O18) CO* refers to the “normal” carbon monoxide ¹²C¹⁶O desorbed from the NEG surface saturated with ¹³C¹⁸O.

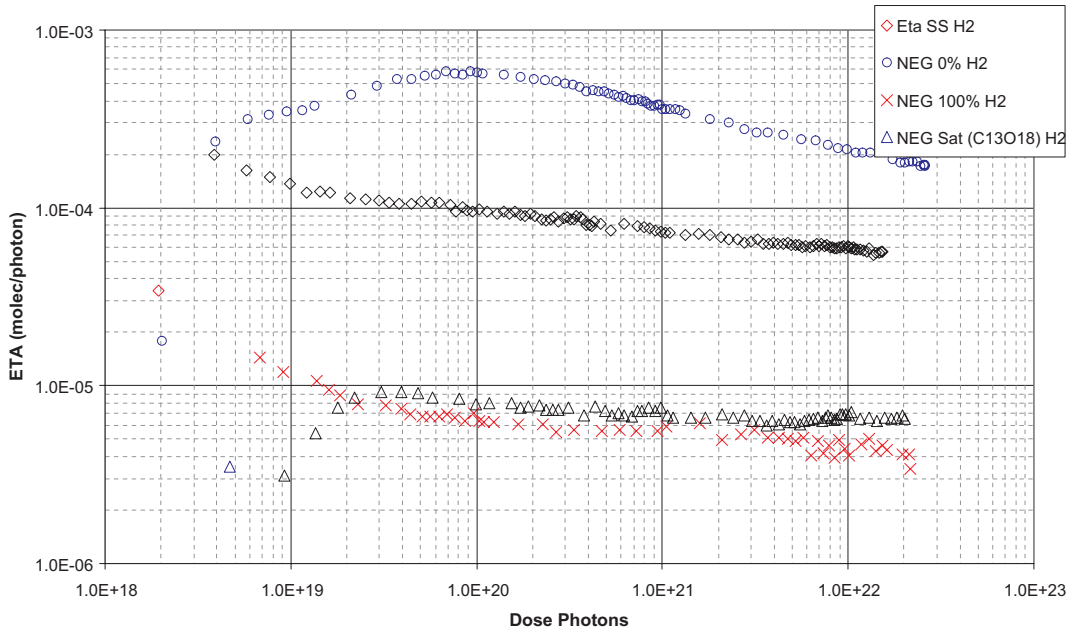


Figure 3: Photodesorption yield of hydrogen from stainless steel (Diamonds) and from NEG St 707, “as received” (Circles), activated at 100% (Crosses), saturated with $^{13}\text{C}^{18}\text{O}$ (Triangles).

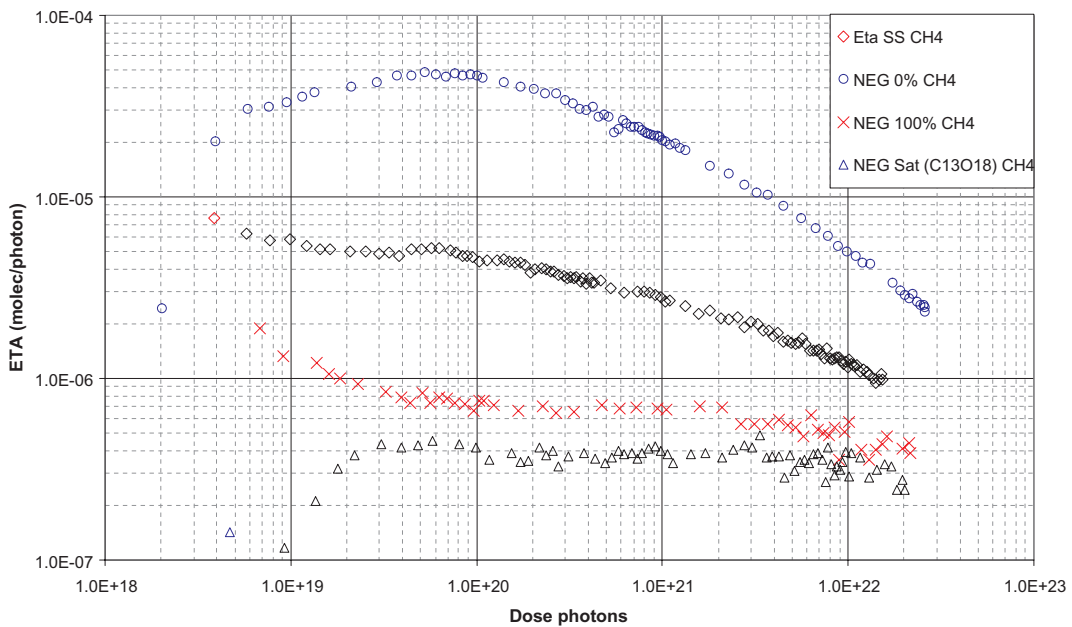


Figure 4: Photodesorption yield of methane from stainless steel and from NEG St 707, “as received” , activated at 100%, saturated with $^{13}\text{C}^{18}\text{O}$.

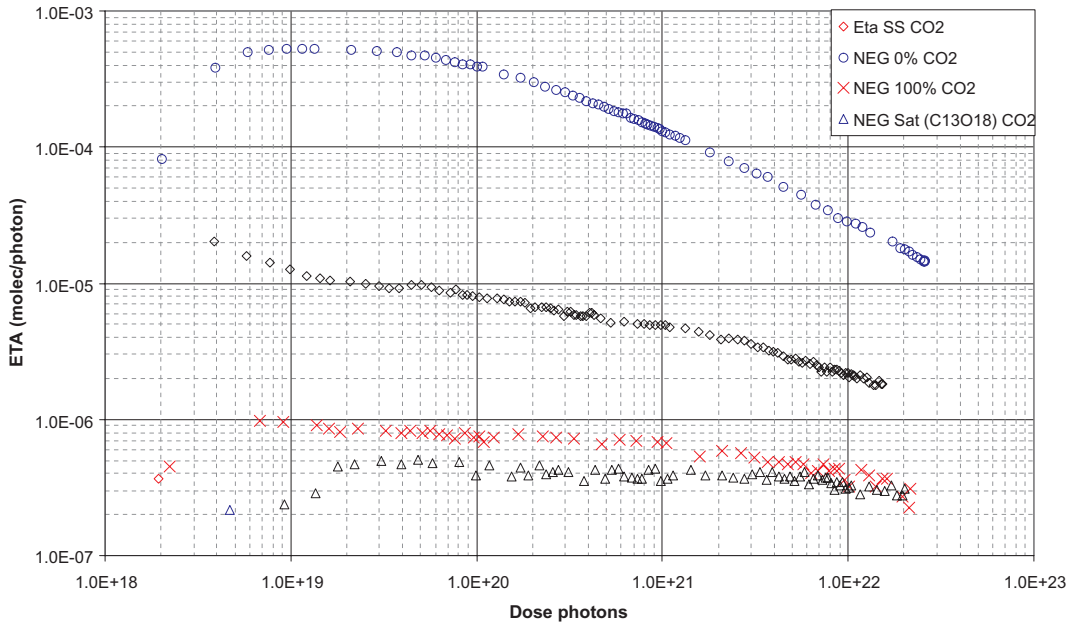


Figure 5: Photodesorption yield of carbon dioxide from stainless steel and from NEG St 707, “as received”, activated at 100%, saturated with $^{13}\text{C}^{18}\text{O}$.

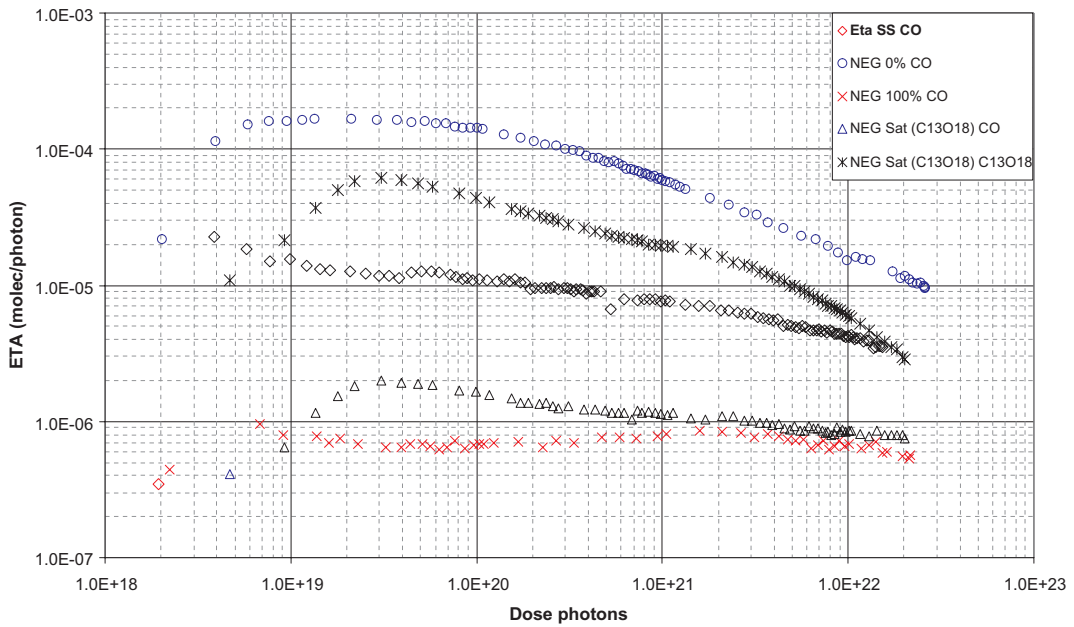


Figure 6: Photodesorption yield of $^{12}\text{C}^{16}\text{O}$ from stainless steel (Diamond) and from NEG St 707, “as received”, activated at 100%, and NEG St 707 saturated with $^{13}\text{C}^{18}\text{O}$ desorbing $^{12}\text{C}^{16}\text{O}$ (Triangles) and $^{13}\text{C}^{18}\text{O}$ (Asterisks).

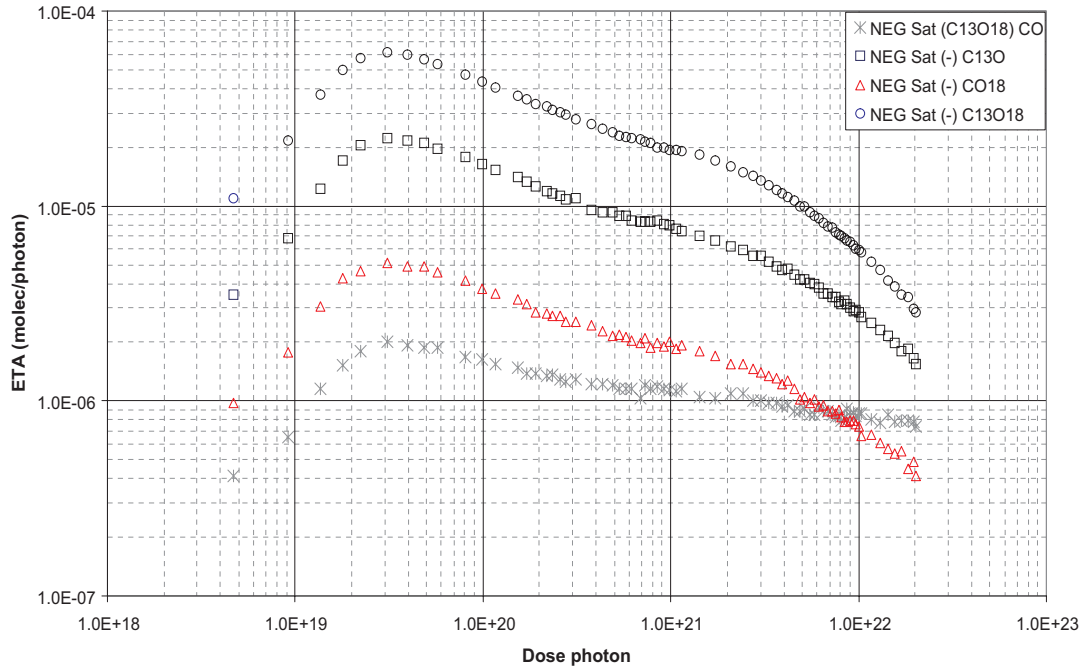


Figure 7: Photodesorption yield of carbon monoxide, $^{12}\text{C}^{16}\text{O}$ (Asterisks), $^{13}\text{C}^{18}\text{O}$ (Circles), $^{13}\text{C}^{16}\text{O}$ (Squares) and $^{12}\text{C}^{18}\text{O}$ (Triangles) from a NEG St 707 saturated by $^{13}\text{C}^{18}\text{O}$.

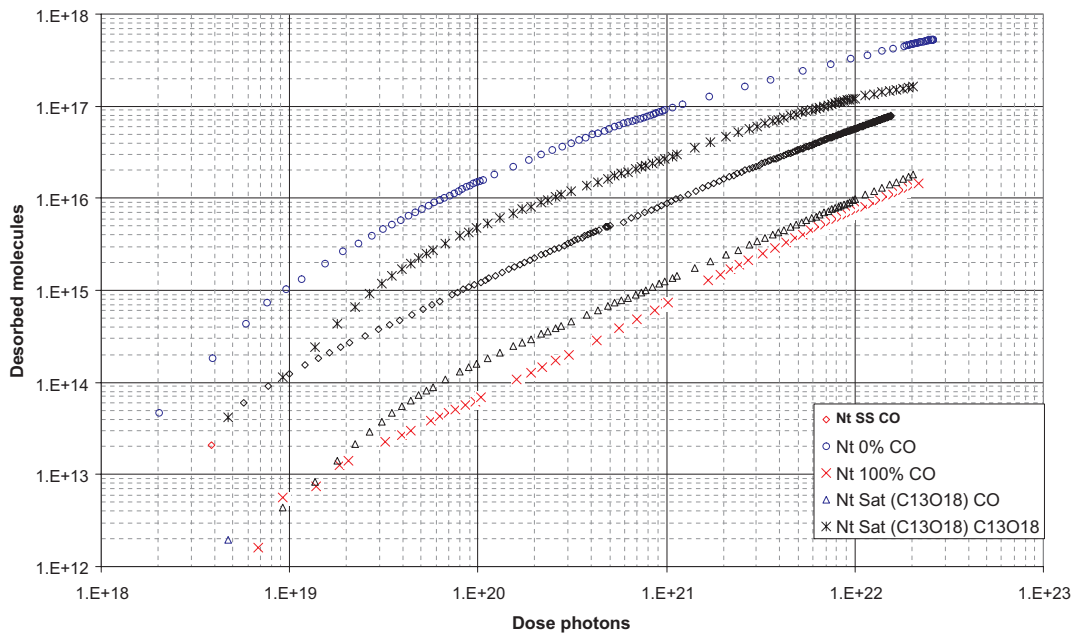


Figure 8: Total number of $^{12}\text{C}^{16}\text{O}$ molecules desorbed from stainless steel (Diamonds) and from NEG St 707, “as received” (Circles), activated at 100% (Crosses), saturated with $^{13}\text{C}^{18}\text{O}$ desorbing $^{12}\text{C}^{16}\text{O}$ (Triangles) and $^{13}\text{C}^{18}\text{O}$ (Asterisks).

6 Discussion

As compared to stainless steel and the non activated NEG, activating the NEG samples introduces an additional pumping speed in the system. As a consequence, desorbed molecules have a finite probability to be re-adsorbed on the activated NEG surface and are therefore not measured by the external gauge. To account for this effect it is necessary to correct the “effective” η values obtained by equation (1) by the pumping speed of the NEG to obtain the real or “intrinsic” PSD yield .

In order to take this re-adsorption effect into account, a Monte Carlo (MC) method, similar to the one described in [2], has been used. This MC takes into account the full geometry of the system from the target to the conductance, Figure 1.

The immediate observation that can be made from the results shown in Figure 3 to 6 is the low PSD yield of the fully activated NEG as compared to the desorption yield of the 300 °C baked stainless steel as well as to the desorption yield of the NEG in the “as received” state.

The reduction factor between the activated NEG and the “as received” NEG is contained between 20 and 50 depending on the gas species. Because of the uncertainty in estimating the parasitic desorption effect, cf § 3, it can, however, not be excluded that the PSD values of the activated NEG St 707, irradiated at RT and at normal incidence, may even be lower than what is shown here.

As a first result we can see that the PSD yield of hydrogen, methane and of carbon dioxide are lower for the saturated NEG than the corresponding values of baked stainless steel, Figure 3, 4 and 5.

In the case of the saturation by $^{13}\text{C}^{18}\text{O}$, it is known that the carbon monoxide can inhibit the adsorption, and hence reduce the pumping of hydrogen and of other gases on a Zr based NEG [3] [8]. By analogy and since the isotope $^{13}\text{C}^{18}\text{O}$ should behave the same as $^{12}\text{C}^{16}\text{O}$ for any chemical reaction this gas should equally block the gettering effect of the St 707. As the reverse of this process, the oxide layer present on the NEG after saturation with carbon monoxide (normal or isotopic) should in turn reduce the PSD yield of other gas species. It would result from this hypothesis that the PSD yield of H_2 , CH_4 , CO_2 should be similar to the one of the fully activated NEG.

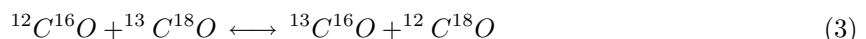
This hypothesis is indeed supported by the observations presented in Figures 3, 4, 5 and 6, which show that the PSD yield for H_2 , CH_4 , $^{12}\text{C}^{16}\text{O}$, CO_2 of the $^{13}\text{C}^{18}\text{O}$ saturated NEG (triangles) are indeed quite similar to the fully activated NEG (crosses).

As a second result Figure 6 shows that a $^{13}\text{C}^{18}\text{O}$ saturated NEG desorbs slightly more $^*\text{C}^*\text{O}$ (Asterisks) than a baked stainless steel surface (Diamonds), but less $^*\text{C}^*\text{O}$ than an “as received” NEG (Circles). Nevertheless, the PSD coefficients for $^{13}\text{C}^{18}\text{O}$ of the saturated NEG become similar to the $\eta_{^{12}\text{C}^{16}\text{O}}$ of the stainless steel after an accumulated exposure of $\sim 10^{22}$ photons of the surface. The “cleaning” slope for the $^{13}\text{C}^{18}\text{O}$ is also more pronounced than that of stainless steel leading to the general conclusion that the NEG will globally desorb less gas than baked stainless steel. The contribution of the $^{12}\text{C}^{16}\text{O}$ coming from the bulk of the NEG, plus the addition of the PSD yields of the other isotopic carbon monoxide ($^{13}\text{C}^{16}\text{O}$ and $^{12}\text{C}^{18}\text{O}$), Figure 7 seems to be insufficient to reverse this behaviour. To put this result in the context of the future LHC vacuum system, a photon dose of 10^{22} photons on the target would be reached typically after 2 hours of operation at normal conditions [2].

One should also take note of the shape of the PSD curves for all the isotopes, Figure 7. All curves start out systematically with a slow initial increase of the η before the actual cleaning of the samples is observed at much higher photon dose. This typical behaviour could not be seen when the NEG was saturated with $^{12}\text{C}^{16}\text{O}$ only [16]. The usual behaviour at room temperature is an initially large PSD yield followed by a gradual, slow decrease, which is due to the cleaning effect of the surface by the photons. One is tempted to attribute this distinct difference to the combined processes of the recombination of initially dissociated atoms of ^{13}C and ^{18}O and the gradual removal of the surface molecules leading to the observed cleaning effect.

The experiments by saturating the surface with $^{13}\text{C}^{18}\text{O}$ had the purpose to determine if there is any recombination between the isotopic atoms ^{13}C and ^{18}O and pre-existing, normal atoms coming from the bulk or present on the surface.

It has been shown in [8] and [9] that $^{12}\text{C}^{16}\text{O}$ is adsorbed dissociatively on a Zr surface. Following this hypothesis the mass peaks between 2 to 50 *amu* have been scanned in order to check if any dissociated elements of $^{13}\text{C}^{18}\text{O}$ were able to recombine with other atoms present in the bulk or on the surface of the NEG. Equation(3) shows the isotopic balance after dissociation, recombination and desorption of the NEG surface.



The recorded spectra show peaks with mass 29 and 30 which can be attributed to $^{13}\text{C}^{16}\text{O}$ and $^{12}\text{C}^{18}\text{O}$. Furthermore some traces of isotopic carbon dioxide could be detected. Unfortunately, a subsequent cross check of the gas supply revealed that these species were already present in the gas bottle. Consequently it was not possible to obtain a conclusive result from this recombination experiment. All what could be confirmed was that pre-deposited molecules are removed during the photon irradiation [2].

Finally it was important to quantify the total number of molecules that can be removed by PSD from the $^{13}\text{C}^{18}\text{O}$ saturated NEG target, Figure 8 (Asterisks), and to compare this result with the cleaned and baked stainless steel target (Diamonds). The stainless steel surface has released approximately 1 ML of $^{12}\text{C}^{16}\text{O}$ molecules at the end of the experiment.

In order to compare these numbers of desorbed molecules from the getter with the stainless steel target, it is necessary to take into account the surface roughness of the NEG St 707. The roughness values of the NEG St 707 was extracted from the pumping speed curve of [6] and [17]. The getter is about 60 times rougher ($R \sim 60$) than the stainless steel used for the experiments. The number of molecules present in 1 ML_{NEG} of the 6.5 cm^2 irradiated area corresponds to $4 \cdot 10^{17}$ molecules². Moreover, taking into consideration the fact that backscattered photons may in addition impinge on the Sleeve (Figure 2), the total number of isotopic molecules ($N_{^{13}\text{C}^{18}\text{O}} + N_{^{13}\text{C}^{16}\text{O}} + N_{^{12}\text{C}^{18}\text{O}}$), [2], desorbed at the end of the irradiation turn out to be $\sim 0.5 \text{ ML}_{NEG}$ which is well below the $1.2 \cdot 10^{19}$ molecules that should have been present on the surface. From this rather crude quantitative estimate one must conclude that the amount of gas which could be released by PSD during an entire run was well below the estimated amount of $^{13}\text{C}^{18}\text{O}$ deposited initially on the surface of the NEG target.

Two explanations can be advanced in order to understand this low number of molecules desorbed from the $^{13}\text{C}^{18}\text{O}$ saturated NEG, as well as the relatively low desorption coefficient as compared with the “as received” NEG.

As a first explanation, one should take into consideration the structure of the St 707. The getter is produced by sintering a powder of ZrVFe alloy onto a constantan ribbon. The nominal thickness of the alloy on the substrate is $70 \mu\text{m}$ [7]. This method results in a very rough but also a very porous getter.

During the saturation process the molecules will chemisorb not only on the visible, exposed surface but will also migrate inside the voids between individual grains and chemisorb on the shadowed surface of these grains. One can characterise the effective surface as a rough surface with many small pores. Since the attenuation length of 200 eV monochromatic radiation in the getter alloy is $\sim 80 \text{ nm}$ [18] this suggests that only a small fraction of the real NEG surface can be reached by the photons and thus can contribute to the PSD process. In other words only a small fraction of the deposited molecules will be available for the desorption process. In addition, this porous structure explains readily the low desorption coefficient of the fully saturated NEG. Since the molecules are trapped inside the confined space of the pores, they may undergo, during the PSD process, a large number of desorption-adsorption events inside the pores before escaping from the surface.

An alternative hypothesis that may explain the relatively low PSD yield and the significantly reduced total number of $^{13}\text{C}^{18}\text{O}$ molecules desorbed during these experiments, is the possibility that in presence of intense photon irradiation atoms diffuse into the bulk of getter alloy leaving the surface in a clean state. To obtain a crude estimate of this effect a comparison with the thermal activation process of the getter has been made. During the activation at a temperature between $300 \text{ }^\circ\text{C}$ and $400 \text{ }^\circ\text{C}$ (the corresponding thermal energies range between 0.05 eV and 0.06 eV) the adsorption sites located on the NEG surface become “free” of molecules. For the NEG, the atoms forming the molecules diffuse inside the bulk in order to minimize their potential energy, and are accumulating inside the bulk of the getter. On the contrary, for conventional materials like stainless steel raising the temperature commonly increases their outgassing rate. It has to be mentioned that for a NEG being at room temperature, the molecules adsorbed ($^{12}\text{C}^{16}\text{O}$, CO_2) on its surface are chemisorbed and do not diffuse inside its bulk, at the exception of hydrogen.

The much larger energy deposited by the SR photons may act locally as a thermal activation process. In other words, it is not unreasonable to expect that photon irradiation would enhance both, the diffusion process into the bulk as well as the desorption rate. One consequence of this process should be that new, free adsorption sites become available on the surface which can act as pumping sites. In this context it is relevant to recall earlier measurements on copper and on stainless steel chambers where a large, permanent pumping speed could be measured after photon irradiation [19] [20] [21].

The hypothesis of radiation stimulated diffusion has been investigated using Auger analysis of the different

²1 ML $\sim 10^{15}$ molecules. cm^{-2} , 1 $\text{ML}_{NEG} = R \times 1 \text{ ML}$

samples and at various stages of irradiation. Unfortunately, with the limited data no conclusive results could be obtained [2].

7 Conclusion

From this study we can conclude that the fully activated NEG desorbs less gas as compared to a 300 °C baked stainless steel surface. This first conclusion is in agreement with previous results obtained with 500 eV [3] and 45 eV [2] critical energy SR radiation.

We also find that a NEG saturated with $^{13}\text{C}^{18}\text{O}$ and then exposed to SR of 194 eV of critical energy desorbs slightly more $^{13}\text{C}^{18}\text{O}$ than baked stainless steel. The η becomes similar after an exposure of $2 \cdot 10^{22}$ photons and if this trend continues, the PSD yield will drop below the stainless steel values for higher doses. In the case of the experimental areas of the LHC, where some NEG will be installed, this results may be of interest to avoid the troublesome preparation of reactivating a NEG which is partially saturated. A dose of 10^{22} photons can be obtained after only a couple of hours of LHC running at nominal condition.

By comparison, in the experiments carried out with 45 eV critical energy SR [2], the $^{12}\text{C}^{16}\text{O}$ desorption coefficient of the $^{12}\text{C}^{16}\text{O}$ saturated NEG was about the same as the PSD coefficient of stainless steel. This difference of behaviour between the two experiments, 45 eV and 194 eV, may be attributed to the harder energy spectrum of the SR, as well as by the higher photon flux impinging the target. However, this last hypothesis seems improbable due to the fact that for the maximum photon flux $\dot{\Gamma}$ the temperature of the target never exceeded 28°C, therefore not inducing any thermal desorption.

During the photon irradiations, it was found that it was not possible to remove the total amount of the pre-deposited $^{13}\text{C}^{18}\text{O}$ molecules from the St 707 surface. The relatively low PSD coefficient of the NEG and the apparent failure of the surface cleaning may be explained by the structure of the St 707 and/or by the possibility that surface atoms may have diffused into the bulk of the NEG during the irradiation.

These two hypotheses merit to be further investigated. This could be done by using getters deposited on the sample surface as thin films offering the advantage that their roughness can be well controlled during the film growth [22].

By saturating a very smooth getter film with isotopically pure $^{13}\text{C}^{18}\text{O}$ gas and by analyzing the composition of the desorbed gas with the RGA it should be possible to obtain reliable information on the recombination process. Determining the integral number of molecules desorbed during irradiation of such films with varying surface roughness should provide information on the speculated roughness effect. Finally a SIMS analysis with its capability to differentiate between isotopes, should provide a reliable test of the atomic diffusion process inside the NEG during the SR irradiation.

8 Acknowledgments

The authors would like to thank Drs. J P. Potier and L. Rinolfi for providing extensive synchrotron radiation beam time and also the team of the EPA operators for their continuous help and for providing the required stable beam conditions. The assistance of Dr V. Baglin for his help in setting up of the experiment is gratefully acknowledged.

References

- [1] David R. Lide, editor. *Handbook of Chemistry and Physics*. 74th edition. CRC PRESS, 1994.
- [2] F. Le Pimpec. *Etude de la Désorption Moléculaire Induite par Transitions Electroniques dans les Surfaces Techniques*. PhD thesis, Université Pierre et Marie Curie Paris 6, 2000. <http://documents.cern.ch/archive/electronic/cern/preprints/thesis/thesis-2000-017.pdf>.
- [3] H.J. Halama and Y. Guo. Non Evaporable Getter Investigation at the National Synchrotron Light Source. *Journal of Vacuum Science and Technology*, A 9(3):2070, 1991.
- [4] T. Kobari et al. NEG Performance under Synchrotron Radiation. Paper presented at the topical conference on vacuum systems for synchrotron light sources - Brookhaven May 1988.

- [5] F. Le Pimpec, O. Gröbner, J.M Laurent. Electron stimulated molecular desorption of a non evaporable Zr-V-Fe alloy getter at room temperature. *Nuclear Instruments and Methods in Physics Research B*, 194 (4):434–442, 2002.
- [6] C. Benvenuti and P. Chiggiato. Pumping Characteristics of the St707 Non-Evaporable Getter (Zr 70 V 24.6-Fe 5.4 wt %). *Journal of Vacuum Science and Technology*, A 14(6):3278, 1996.
- [7] The SAES Getters Group public documentation. St 707 Non Evaporable Getters Activatable at Low Temperatures.
- [8] P.J. Goddard J.S. Foord and R.M. Lambert. Adsorption and Absorption of Diatomic Gases by Zirconium: Studies of the Dissociation and Diffusion of CO, NO, N₂, O₂ and D₂. *Surface Science*, 94:339–354, 1980.
- [9] I. Vedel, L. Schlapbach. Surface Reactivity of Zr-V-Fe Getter Alloys exposed to H₂O CO and O₂ at 300 and 700 K. *Journal of Vacuum Science and Technology*, A 11(3):539, 1993.
- [10] A.G. Mathewson. The Effect of Cleaning and Other Treatments on The Vacuum Properties of Technological Materials Used in Ultra-High Vacuum. Technical report, CERN-LEP-VA 87-63, 1987.
- [11] P.A Redhead. The First 50 Years of Electron Stimulated Desorption (1918-1968). *Vacuum*, 48 (6):585, 1997.
- [12] R.D. Ramsier and J.T. Yates Jr. Electron-Stimulated Desorption: Principles and Applications. *Surface Science Reports*, 12 (6-8):243, 1991.
- [13] D. Lichtman, Y. Shapira. Photodesorption: A Critical Review. *CRC Critical Reviews in Solid State and Materials Sciences*, 8:93, 1978.
- [14] D. Lichtman. Mechanisms of Desorption Due to Electrons or Photons. *Surface Science*, 90:579–587, 1979.
- [15] M. Akbulut et al, surf. Elastic and inelastic process in the interaction of 1-10 eV ions with solids : ion transport through surface layers. *Surface Science Reports*, 28:177, 1997.
- [16] F. Le Pimpec. Molecular Desorption Induced by Photons on NEG St 707 at Room Temperature. Technical report, CERN-LHC-VAC 98-24, 1998.
- [17] Z. Liu J.M Laurent. Mesures de Vitesses de Pompage d’un NEG St 707. private communication.
- [18] X-ray interaction with matter; Lawrence Berkeley Laboratory from [23]. http://www-cxro.lbl.gov/optical_constants/atten2.html.
- [19] O. Gröbner, and A.G. Mathewson, P.C Marin. Gas Desorption from an OFHC Copper Vacuum Chamber by Synchrotron Radiation. *Journal of Vacuum Science and Technology*, A 12(3):846, 1994.
- [20] C. Herbeaux, P. Marin, V. Baglin, O. Gröbner. Photon Stimulated Desorption of an Unbaked Stainless Steel Chamber by 3.75 KeV Critical Energy Photons. *Journal of Vacuum Science and Technology*, A 17(6):635, 1999.
- [21] C.L. Foerster, C. Lanni, K. Kanazawa. Measurements of photon stimulated desorption from thick and thin oxide of KEK B collider copper beam chambers and a stainless steel beam chamber. *Journal of Vacuum Science and Technology*, A 19(4):1652, 2001.
- [22] C. Benvenuti and al. A Novel Route to Extreme Vacua : the Non Evaporable Getter Thin Film Coatings. *Vacuum*, 53:219, 1999.
- [23] B.L. Henke, E.M. Gullikson, and J.C. Davis. X-ray interactions: photoabsorption, scattering, transmission, and reflection at E=50-30000 eV, Z=1-92. *Atomic Data and Nuclear Data Tables*, 54 (2):181–342, 1993.